New magnetic-resonance-imaging-visible poly(e-caprolactone)-based polyester for biomedical applications

Sebastien Blanquer, Olivier Guillaume, Vincent Letouzey, Laurent Lemaire, Florence Franconi, Cédric Paniagua, Jean Coudane, Xavier Garric

New magnetic-resonance-imaging-visible poly(ε-caprolactone)-based polyester for biomedical applications

Sebastien Blanquer [a], Olivier Guillaume [a], Vincent Letouzey [a,b], Laurent Lemaire [c,d], Florence Franconi [c], Cedric Paniagua [a], Jean Coudane [a], Xavier Garric [a,⇑]

[a] Max Mousseron Institute of Biomolecules (IBMM), UMR CNRS 5247, Universities Montpellier I and II, Faculty of Pharmacy, 15 Av. C. Flahault, Montpellier F34093, France
[b] Obstetrics and Gynaecology Department, Caremeau University Hospital, Nîmes, France
[c] LUNAM University, UMR-S646, Angers F49933, France
[d] INSERM, U646, Micro et nanomédecines Biomimétiques – MINT, Angers F49933, France

article info

Article history:
Received 1 August 2011
Received in revised form 3 November 2011
Accepted 4 November 2011
Available online 11 November 2011

Keywords:
Polycaprolactone
MRI
Gadolinium
Prosthesis
DTPA

abstract

A great deal of effort has been made since the 1990s to enlarge the field of magnetic resonance imaging. Better tissue contrast, more biocompatible contrast agents and the absence of any radiation for the patient are some of the many advantages of using magnetic resonance imaging (MRI) rather than X-ray technology. But implantable medical devices cannot be visualized by conventional MRI and a tool therefore needs to be developed to rectify this. The synthesis of a new MRI-visible degradable polymer is described by grafting an MR contrast agent (DTPA-Gd) to a non-water-soluble, biocompatible and degradable poly(ε-caprolactone) (PCL). The substitution degree, calculated by ^{1}H nuclear magnetic resonance and inductively coupled plasma-mass spectrometry, is close to 0.5% and proves to be sufficient to provide a strong and clear T1 contrast enhancement. This new MRI-visible polymer was coated onto a commercial mesh for tissue reinforcement using an airbrush system and enabled in vitro MR visualization of the mesh for at least 1 year. A stability study of the DTPA-Gd-PCL chelate in phosphate-buffered saline showed that a very low amount of gadolinium was released into the medium over 52 weeks, guaranteeing the safety of the device. This study shows that this new MRI-visible polymer has great potential for the MR visualization of implantable medical devices and therefore the post-operative management of patients.

1. Introduction

Polymeric biomaterials are being increasingly used for biomedical applications as implantable devices or drug delivery systems [1–3]. As these biomaterials offer a great variety of structures, and therefore possess a broad range of properties, they can be used in a host of applications. One of the most important applications in the biomedical field is the use of these polymers for medical devices, especially prostheses. Such materials can be used for permanent or temporary applications, depending on their structure [4–6]. Unfortunately, all these polymeric materials are transparent to X-rays and are invisible using magnetic resonance imaging (MRI). This inability to visualize implanted material restricts any evaluation of tissue integration and post-operative fixation, and any determination of fate in the body [7].

A radio-opaque poly(ε-caprolactone) (PCL)-based aliphatic polyester has been developed in our laboratory in which a covalent link has been formed between a radio-contrast dye (typically iodine) and the polymeric backbone [8].

MRI is a non-ionizing technique that is widely used in clinical practice, mainly because of its non-invasive nature, its capability to produce high-definition images and its ability to depict pathological tissues [9–12]. Image contrast is often enhanced by using contrast agents [13,14] and this approach may be used to visualize polymeric material. In a recent report, Kramer et al. have reported the synthesis of surgical textile implant loaded with iron oxide nanoparticles during the polyvinylidene fluoride threads extrusion [15]. The resulting material was visualized by MRI using the positive-contrast inversion recovery with on-resonant water suppression sequence [16]. Positive contrast may also be gained using conventional MRI sequences if paramagnetic agents, such as gadolinium salts Gd(III), are used [17]. Unfortunately, gadolinium salts are toxic and must be chelated [18]. Of all gadolinium chelates, diethylenetriaminepentaacetic acid (DTPA) is the most frequently used in medical imaging [19].

Several methods have been reported in the literature to design macromolecular DTPA-Gd complexes. Applications of these new contrast agents in blood pool imaging are focused on the

* Corresponding author. Tel.: +33 467548564; fax: +33 467520898.
E-mail address: xavier.garric@univ-montp1.fr (X. Garric).

modification of the pharmacokinetics [20], through chelating structures grafted onto water-soluble macromolecules [18,21–26]. However, these water-soluble macromolecular complexes are rapidly excreted and cannot be used for the MRI visualization of non-water-soluble implanted devices.

Very few studies have been conducted on the conjugation of Gd(III) chelates to hydrophobic polymers. In some cases the contrast agent is dispersed within a polymeric matrix [27]. It can diffuse out of the device and therefore enables only transitory visualization, as for example with PLAGA microspheres [28]. In order to overcome this drawback, a chelate of the contrast agent should be covalently linked on a polymer chain, but this approach requires the functionalization of the polymeric backbone prior to the addition of the chelate. Jiang et al. [29] mentioned a surface modification of a polymeric plate by plasma treatment with hydrazine followed by reaction of DTPA on the amine group. However, the resulting hydrolysable amide bond may not be suitable for the long-term visualization requirement. In addition, this method is known to induce possible reactive pendant function rearrangements on the surface, which can decrease the material's reactivity [30,31]. Another study referred to a hydrophobic poly(styrene-maleic acid) (SMA) copolymer grafted onto a gadolinium (HEDTA (hydroxylethylenediaminetetraacetic acid)) chelating agent [32]. In this case a potentially hydrolysable ester bond is created between the chelating agent and the polymer and this again may not be suitable for long-term visualization.

The purpose of the work described herein was to synthesize a new biodegradable MRI-visible polymer in order to provide a tool for surgeons to locate implanted polymeric prostheses. This new polymer needed to ensure that medical devices can be visualized long term by MRI: (i) the polymer must be non-water-soluble in order to remain immobilized on the surface, (ii) it should degrade slowly to provide at least 1-year post-operative MRI visualization, without permanently modifying the characteristics of the medical device, (iii) visualization must be possible until the polymer has completely degraded. Thus, the contrast agent should be linked to the monomeric units in a non-cleavable manner to be finally released concomitantly with the degradation products. To meet these specific requirements, a chelate of a contrast agent (DTPA) was grafted onto a non-water-soluble, degradable and biocompatible polymer by a covalent and non-cleavable bond. Poly(ε-caprolactone) (PCL) was selected for its biocompatibility and FDA approval, and because this polymer is known to be slowly degraded in the human body [4–6]. This polymer is not functionalized, but we have previously described a rapid, easy and versatile method to chemically activate PCL chains in a polycarbanionic form [33]. Briefly, this activation is achieved by using lithium diisopropylamide (LDA) as a non-nucleophilic strong organic base to remove one of the hydrogen atoms at the α-position on the carbonyl groups. In a second step, electrophilic reactants are then bound to the carbanionic sites.

Here, in this present study, we describe the synthesis of a new MRI-visible polymer based on the grafting of a DTPA derivative onto activated PCL, followed by the complexation of Gd^{3+} onto the grafted DTPA. The characterization of all compounds, by-products and final polymer are reported herein. In addition, the potential of this MRI-visible polymer for biomedical applications was investigated by (i) assessing the stability of the Gd^{3+} polymeric complex and the polymer coating on a polypropylene mesh, (ii) experimentally determining the device's MRI visibility and its cytocompatibility.

2. Materials and methods

PCL (Mn = 42,500 g mol^{-1}; Mw 65,000 g mol^{-1}) was obtained from Aldrich (St Quentin Fallavier, France), benzyl alcohol (purity = 99%) and palladium on activated carbon (10% Pd) were purchased from ACROS (Gell, Belgium). $MgSO_4$ and diethylenetriaminepentaacetic acid dianhydride (DTPA-diA) were supplied by Carlo Erba (Milan, Italy) and were used as received.

Lithium di-isopropylamide (LDA) (2 M in tetrahydrofuran/n-heptane); gadolinium(III) chloride hexahydrate, (99%), thionyl chloride ($SOCl_2$), dried tetrahydrofuran (THF); and dichloromethane, diethyl ether, methanol, dry dimethylsulfoxide were purchased from Sigma-Aldrich (St Quentin Fallavier, France). All chemicals and solvents were used without further purification, except THF, which was treated over benzophenone sodium until a deep blue color was obtained, and then distilled.

Polymer molar masses were determined by size exclusion chromatography (SEC) on a Waters Inc. system fitted with a PLgel 5 μm mixed-C (60 cm) (Polymer Laboratories, Les Ulis, France) column as stationary phase and a Waters 410 refractometric detector, eluted with THF at 1 ml min^{-1}. Typically, samples were dissolved in THF at 10 mg ml^{-1} and filtered through a Millex®-FH PTFE filter, pore size 0.45 μm (Millipore Corporation, Billerica, MA, USA) and 20 μl of the polymer solution were injected. The SEC was calibrated with poly(styrene) standards. A Waters PDA 2996 photodiode-array detector was added on-line for the specific detection of aromatic groups.

ATR-FTIR spectra were obtained on polymeric films cast on NaCl and recorded on a Perkin–Elmer Spectrum 100 FT-IR spectrometer using attenuated total reflectance (ATR).

^1H NMR spectra were recorded in d_6-DMSO on an AMX300 Bruker spectrometer operating at 300 MHz. Chemical shifts were expressed in ppm with respect to tetramethylsilane (TMS).

Relaxation times for polymers dissolved in d_6-DMSO were measured on an AMX400 Bruker spectrometer operating at 400 MHz. T1 measurements were obtained using T1 inversion/recovery sequence. This analysis was carried out at 80 °C to facilitate the molecular mobility of the polymer.

Gd^{3+} was quantified using an Element XR sector field ICP-MS (inductively coupled plasma-mass spectrometry) at Géosciences in Montpellier (Montpellier II University). Internal standardization used an ultra-pure solution enriched with indium.

2.1. Synthesis and characterization of the MRI-visible polymer (DTPA-Gd-PCL)

2.1.1. Synthesis of benzylated DTPA (Bn_2-DTPA)

Commercial DTPA dianhydride (14 mmol, 5 g) was dispersed in DMSO (20 ml) and benzyl alcohol (35 mmol, 3.6 ml) was added dropwise for complete dissolution of the mixture within a few hours. The reaction was monitored by infra-red analysis until complete disappearance of the anhydride band at 1820 cm^{-1}. After 5 h the DMSO was evaporated off and the residue precipitated in diethyl ether before being washed several times with diethyl ether.

2.1.2. Chlorination of Bn_2-DTPA (Bn_2-DTPA-Cl)

Bn_2-DTPA (5.3 mmol, 3 g) was dissolved in thionyl chloride (5 ml) and the reaction conducted at room temperature for 2 h under a flow of argon. Thionyl chloride was then evaporated under vacuum. Bn_2-DTPA-Cl was used immediately for the next reaction without any further purification.

2.1.3. Reaction of Bn_2-DTPA-Cl with PCL (Bn_2-DTPA-PCL)

Typically, PCL (26.3 mmol, 3 g) was dissolved in anhydrous THF (200 ml) by stirring in a reactor that had previously been dried overnight. The solution was carefully kept under a flow of dry argon at —40 °C. A 2 M LDA solution (35 mmol, 17.5 ml) was poured through a septum, while stirring, for 30 min. A solution of Bn_2-DTPA-Cl (5 mmol, 3 g) in dry THF was then poured into the mixture. After 30 min of reaction, the mixture was neutralized with

an aqueous solution of 0.1 N HCl to a pH of between 2 and 3, and extracted twice with dichloromethane (200 ml). The combined organic phases were washed with distilled water (200 ml) and dried on anhydrous $MgSO_4$. After filtration, the dichloromethane was partially evaporated off in a vacuum and Bn_2-DTPA-PCL was precipitated in methyl alcohol. Finally, dialyses were carried out using Spectra/Por membrane tubing (cut-off: 3500 Da).

2.1.4. Deprotection of carboxylic acid groups

Bn_2-DTPA-PCL (8 mmol, 1 g) was dissolved in THF (50 ml) containing a 10% (100 mg) suspension of Pd/C. The reactor was placed under 5 bars of H_2 pressure for 3 days at room temperature with vigorous stirring. The catalyst was removed by filtration on celite. The solvent was partially evaporated off in a vacuum and deprotected DTPA-PCL was precipitated in methyl alcohol.

2.1.5. Complexation of gadolinium

DTPA-PCL (8 mmol, 1 g) was dissolved in DMSO (5 ml) and a solution of gadolinium trichloride (0.8 mmol, 302 mg) in DMSO (1 ml) was added dropwise. The complexation was carried out for 48 h at room temperature while stirring. The DMSO was then evaporated off, CH_2Cl_2 (50 ml) was added and the organic phase was washed twice with H_2O (25 ml). The organic phase was dialyzed against a mixture of $MeOH/CH_2Cl_2$ 50/50 v/v. Finally, the DTPA-Gd-PCL complex was recovered after precipitation in methyl alcohol.

2.1.6. Titration of gadolinium

15.8 mg of DTPA-Gd-PCL were mineralized at 150 °C in nitric acid (70%) for 12 h. The solution was then diluted in water (1/1000) and analyzed by ICP-MS.

2.2. MRI evaluation

2.2.1. Formulation of MRI-visible meshes

A 3 × 3 cm monofilament polypropylene mesh (PP mesh, kindly donated by COVIDIEN (Trevoux, France)), was coated using an Infinity Airbrush system supplied by Harder & Steenbeck (Oststeinbek, Germany). A solution of DTPA-Gd-PCL in acetone (1% w/v) was sprayed under 3 bars of argon pressure onto the polypropylene mesh from a distance of 5 cm. The mesh was dried in a vacuum overnight and weighed to measure the amount of coated polymer. The surface appearance of the coated mesh was characterized by environmental scanning electron microscopy (ESEM) (Philips XL30 ESEM, FEI Company, Hillsboro, WA) at a 10 kV accelerating voltage and by optical microscopy (Stereomicroscope Leica MZ6 connected to an EC3 digital camera, Nanterre, France).

2.2.2. MR imaging protocol

MR imaging experiments were performed on a Bruker Avance DRX system (Bruker Biospin SA, Wissembourg, France) operating on a Paravision (version 4.0) software platform (Bruker Biospin SA, Wissembourg, France). The system was equipped with a 150 mm vertical super-wide-bore magnet operating at 7 T, a 84 mm inner diameter shielded gradient set capable of 144 mT m^{-1} maximum gradient strength and a 30 mm diameter birdcage resonator. Powders (5 mg), modified or native PP meshes (1 cm^2) were embedded in a degassed 1% (w/w) agarose gel prior to imaging. Gadolinium-free samples corresponded to a PP mesh and to a PP mesh coated with DTPA-PCL. A positive control was prepared by coating the mesh with Magnevist®. To test signal enhancement, T1 weighting was introduced into the MR images using an inversion pulse [34] in rapid three-dimensional (3-D) acquisition with relaxation enhancement (RARE) sequence (TR = 2000 ms; mean echo time (TEm) = 31.7 ms; RARE factor = 8; FOV = 3 × 3 × 1.5 cm; matrix 128 × 128 × 64). Inversion time was set at 1300 ms, sufficient to allow canceling of the embedding gel.

2.2.3. Stability studies

Coated meshes were immersed in phosphate-buffered saline (PBS) (Ref 70011, Gibco) at 37 °C with stirring at 130 rpm (Heidolph Uniamx 1010) for 12 months. Aliquots of PBS solution were taken at scheduled time points and directly analyzed by ICP-MS to measure the amount of gadolinium released into the PBS. A positive control consisted of a mesh coated successively by Magnevist® then PCL. At the end of the stability study, the gadolinium still grafted onto the coated meshes was quantified after DTPA-Gd-PCL degradation in HNO_3 as previously described.

2.2.4. In vitro cytocompatibility

The in vitro toxicity of the MRI-visible polymer was assessed by measuring the adhesion and proliferation of human fibroblasts (HFBs) on the surface of polymer films. The airbrush was used to spray PCL and DTPA-Gd-PCL directly onto the bottom of untreated 24-well tissue culture plates (Falcon™, Becton Dickinson, Le Pont De Claix, France) that were then dried in a vacuum overnight. Adhesion after 15, 30 and 60 min and proliferation after 1, 4 and 7 days were evaluated by MTT assay. In these adhesion and proliferation tests, 50,000 or 20,000 HFB, respectively, were seeded in triplicate into 1 ml of culture medium on the polymer surfaces. A polystyrene tissue culture plate (TCPS) was used as control (Cellstar®, Greiner Bio-One, Courtaboeuf, France). At scheduled time points, all non-adherent cells were removed from the culture medium, the plate was washed with Dulbecco's phosphate buffered saline (DBPS), and an MTT solution (250 µl, 1 mg ml^{-1} in DPBS) was added. After 3 h of MTT incubation, the reagent was removed, the plate was washed with DPBS, and isopropyl alcohol was added to solubilize the formazan, which was quantified at 570 nm on a spectrophotometer (Victor™*X*3multilabel plate reader, PerkinElmer).

All data points and standard deviations correspond to measurements done in triplicate. Cell adhesion and proliferation results were tested by one-way analysis of variance (ANOVA) followed by a comparison of the means using the Student–Newman–Keuls multiple range test. Statistical significance was set at $p < 0.05$.

To complete this study, an investigation – by live and dead staining and observations by scanning electron microscopy (SEM) – was conducted of the morphology and viability of the cells on the coated meshes (obtained by the airbrush technique using the protocol already described) and compared with those of the cells on native meshes.

Briefly, disks (diameter = 1.5 cm) of native polypropylene meshes (PP mesh), DTPA-Gd-PCL and genuine PCL coated meshes were stirred for 2 h in a roller mixer at 33 rpm (supplied by Labomoderne, Paris, France) at 37 °C in tubes of culture medium containing 400,000 HFB ml^{-1}. The meshes were then removed, washed with DPBS to eliminate non-adherent cells, and placed in untreated 24-well tissue culture plates. After 5 and 10 days, a PromoKine live/dead cell staining kit (PromoCell GmbH, Heidelberg, Germany) was used to determine viability: 250 µl of live and dead stain was added and the mixture was incubated with the meshes at 37 °C for 15 min. Cell viability was observed under a TE300 microscope fitted with a DMX1200 digital camera (Nikon, Tokyo, Japan).

The meshes were further examined by SEM (Hitachi 400, Krefeld, Germany). After 5 and 10 days, the meshes were removed from the culture medium and washed. Cells were fixed with 3.3% glutaraldehyde in milloning phosphate buffer pH 7.2 for 1 h at room temperature, followed by washings in milloning buffer. Fixed samples were dehydrated in successive ethanol baths graded from 30% to 70%, followed by critical point drying with CO_2. The meshes were then sputter coated with ≈ 10 nm of gold film then examined under SEM using a lens detector with an acceleration voltage of 10 kV at calibrated magnifications.

3. Results and discussion

3.1. Synthesis and characterization of the MRI-visible polymer

DTPA was preactivated in an acyl chloride form (Bn_2-DTPA-Cl) and reacted on the macropolycarbanion derived from PCL to yield MRI-visible DTPA-Gd-PCL. The DTPA-Gd-PCL synthesis process is presented in Scheme 1 (only substituted units are shown). As DTPA is insoluble in organic solvents, it needed to be modified before the reaction. To do this, DTPA dianhydride (1) was esterified with benzyl alcohol in a quantitative yield to give Bn_2-DTPA, which is soluble in organic solvents (i.e. THF) as well as in thionyl chloride, which was used as a solvent in the next step.

Bn_2-DTPA (2) purity was checked by HPLC and its structure was determined by ^{1}H NMR (Supplementary data 1) and ESI-MS ($[M+H]^+$ = 574.3 Da).

NMR peak assignments for Bn_2-DTPA-were as follows: 2.9 ppm (m, 8H, CH_2–N); 3.4 ppm (s, 6H, CH_2–COOH); 3.6 ppm (s, 4H, CH_2–COO–Bn); 5.1 ppm (s, 4H, CH_2–Ph); 7.3 ppm (m, 10H, aromatic protons).

Bn_2-DTPA was then activated by reaction with thionyl chloride at room temperature. The reaction was monitored by FTIR using the acid chloride band at 1795 cm^{-1} in the activated Bn_2-DTPA-Cl (3) (Supplementary data 2).

As Bn_2-DTPA-Cl is unstable, it was used immediately for the next step without further purification, after evaporation of the thionyl chloride. The presumed structure is composed of three acyl chloride groups, but the number of acyl chloride groups on DTPA was not determined.

At the same time, the macropolycarbanion based on PCL (5) was prepared as described in a previous procedure [33], by the reaction of LDA on PCL (4) in THF at a low temperature.

Bn_2-DTPA-Cl (3) was then reacted on the macropolycarbanion as described in the experimental part to yield Bn_2-DTPA-PCL (6), which was recovered by precipitation in methyl alcohol then filtered, washed with cold methyl alcohol, dried under vacuum

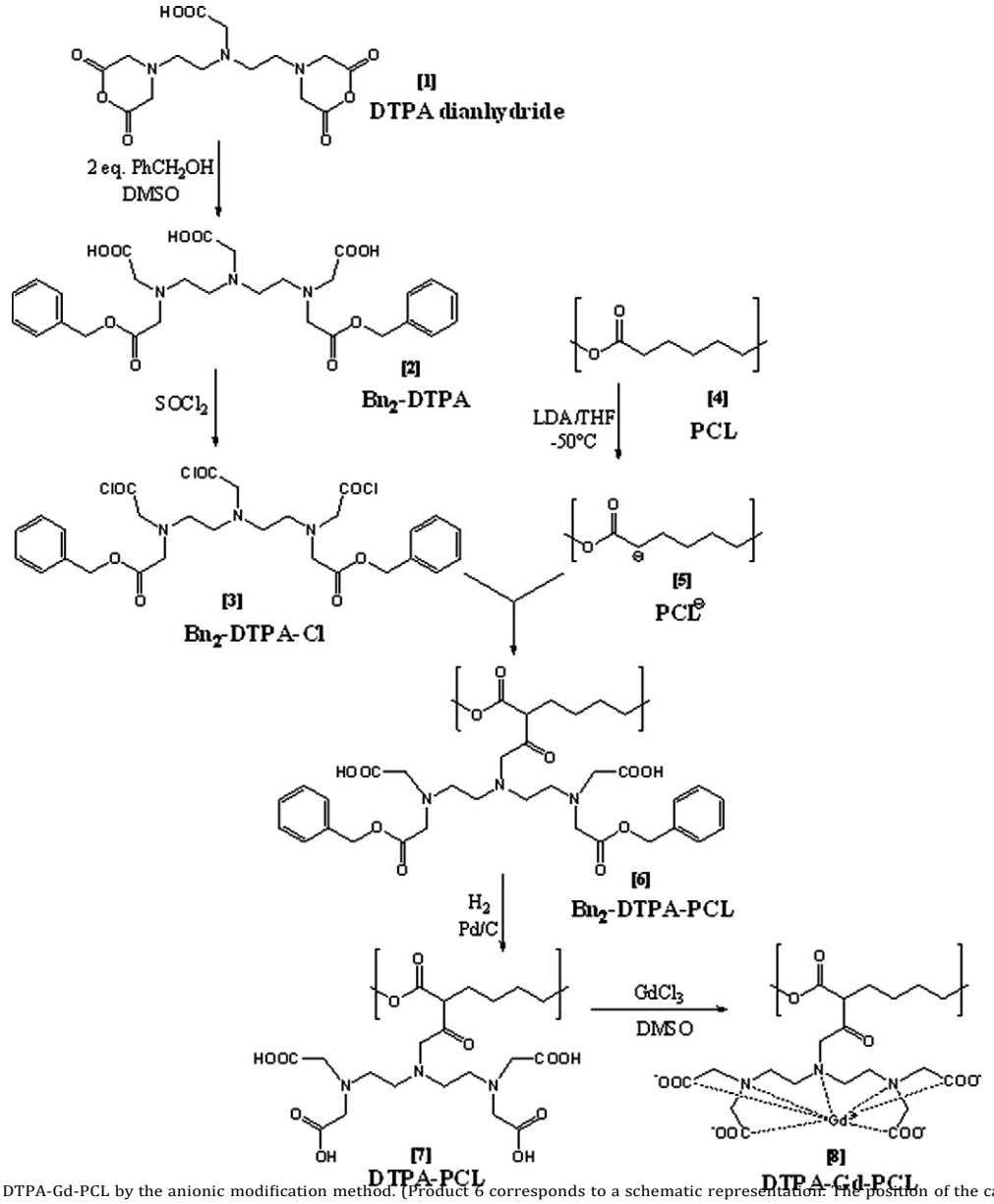

Scheme 1. Synthesis of DTPA-Gd-PCL by the anionic modification method. (Product 6 corresponds to a schematic representation. The position of the carboxylic acid functions obtained after the reaction was not determined.)

and purified by dialysis in CH_2Cl_2/MeOH using tubes with a cut-off ≈3500 Da.

Bn_2-DTPA-PCL purity and molar masses were determined by size exclusion chromatography (SEC) with dual refractometric/PDA detection. The refractometer detects all species whereas PDA provides the UV spectrum of the compound and detects the presence of aromatic chromophores on the polymer backbone. 3-D SEC traces of crude and purified Bn_2-DTPA-PCL are shown in Fig. 1. These data show that: (i) polymer (retention time 15.5 min) absorbed at a wavelength above 250 nm, conclusively demonstrating that grafted benzyl groups are present on the polymeric skeleton (genuine PCL does not absorb at this wavelength); (ii) UV-absorbing small molecules, detected at a retention time of around 26 min, are present in the crude compound. After purifying by three successive dialyses in CH_2Cl_2, no residual UV-absorbing small molecules were observed in the purified Bn_2-DTPA-PCL (Fig. 1A).

The number average molecular mass of Bn_2-DTPA-PCL (6) was 20 kDa instead of 42 kDa for genuine PCL. This decrease stems from a break in the PCL chain during formation of the macropolycarbanion [33].

NMR peak assignments for Bn_2-DTPA-PCL (Fig. 2) are as follows: 1.3 ppm (m, 2H, CH_2–CH_2–CH_2–O); 1.5 ppm (m, 4H, CO–CH_2–CH_2–CH_2–CH_2–CH_2–O); 1.9 ppm (m, 2H, CH_2–CHR–CO); 2.2 ppm (m, 2H, CH_2–CO); 4.0 ppm (m, 2H, CH_2–O); 4.3 ppm (m, 2H, CH_2–O); 5.1 ppm (s, 4H, CH_2–Ph); 7.3 ppm (m, 10H, CH aromatic).

The substitution degree was calculated from the ^{1}H NMR ratio:

$$Sd = \frac{OCH_2 \text{protons of PCL}}{\text{Aromatic protons}} \times \frac{\text{integration of aromatic peak}(\delta 7{:}3\ \text{ppm})}{\text{integration of } OCH_2 \text{peak of PCL}(\delta 4\ \text{ppm})}$$

Considering that all the aromatic species are derived from Bn_2-DTPA-PCL in the purified compound (see above), the substitution degree is 0.5–2%. This low substitution ratio (usually around 10% with this method) is probably a consequence of both steric hindrance and the instability of Bn_2-DTPA-Cl, which is rapidly hydrolyzed.

To obtain a chelating effect, Bn_2-DTPA-PCL needed to be deprotected in order to recover carboxylic acid groups. Benzyl esters were cleaved by catalytic hydrogenolysis in THF, in the presence of Pd (10%) on charcoal. The efficiency of the deprotection was checked by ^{1}H NMR, which showed that all benzyl groups had disappeared from DTPA-PCL (7). The number average molecular mass of DTPA-PCL was 17 kDa and polydispersity index was 2.

DTPA-PCL (8 mmol, 1 g) was dissolved in DMSO (5 ml) and a solution of gadolinium trichloride (0.8 mmol, 302 mg) in DMSO (1 ml) was added dropwise. The complexation was carried out for 48 h at room temperature while stirring. The DMSO was then evaporated off, CH_2Cl_2 (50 ml) was added and the organic phase was washed twice with H_2O (25 ml).

The organic phase was dialyzed against a mixture of MeOH/CH_2Cl_2 50/50 v/v. Finally, the DTPA-PCL complex was recovered after precipitation in methyl alcohol.

The last stage of the synthesis consisted complexing with gadolinium, which was carried out by reacting excess $GdCl_3$ with DTPA-PCL (substitution degree≈1.5%) in DMSO at room temperature. Free gadolinium was eliminated by successive washings with H_2O and dialysis in MeOH/CH_2Cl_2 50/50 until no gadolinium was detected by inductively coupled plasma-mass spectrometry (ICP-MS). The amount of gadolinium chelated to the DTPA-Gd-PCL was measured by ICP-MS. A substitution ratio of 0.3–0.8% was obtained, showing that only ≈20–55% of the gadolinium had chelated to the grafted DTPA. The incompatibility of the water-soluble $GdCl_3$ salt and the hydrophobic polymer may explain this poor complexation ratio.

3.2. MR characterization

3.2.1. DTPA-Gd-PCL relaxation time T1 measurements

The effect of grafted gadolinium was measured by determining the T1 relaxation time for hydrogen atoms on the PCL backbone. As expected, data in Fig. 3 show that the longitudinal relaxation time T1 of the hydrogen atoms on DTPA-Gd-PCL was significantly lower than that in genuine PCL. Moreover, T1 decreased concomitantly with the gadolinium substitution ratio on the PCL skeleton. With regard to the protons on the methylene in the ε-position (Fig. 3a, CH_2–CH_2–CH_2–O), T1 varied from ≈ 1.5 s in genuine PCL to 0.85 s in DTPA-Gd-PCL with a 0.3% substitution ratio and to 0.59 s in DTPA-Gd-PCL with a 0.8% substitution ratio. The same impact of gadolinium complexation was also observed for the other protons in DTPA-Gd-PCL.

3.2.2. MR-imaging of DTPA-Gd-PCL

Fig. 4 illustrates the T1 signal enhancement provided by DTPA-Gd-PCL (substitution ratio of 0.3%) in the form of a powder and after being coated onto a commercial mesh used in the repair of genital prolapse. Negative controls for the powder consisted of DTPA-PCL and genuine PCL, whereas a positive control was based on a Magnevist® solution. The negative controls did not elicit any T1 enhancement, while intense T1 effects were observed for both the positive control (Magnevist®) and DTPA-Gd-PCL. Because the Magnevist® diffused in the gel, a positive effect was observed for the entire medium. In the case of the DTPA-Gd-PCL sample, the grafted contrast agent elicited a significant T1 effect that was localized on the polymer powder area, without any diffusion into the medium.

DTPA-Gd-PCL was then coated onto commercial polypropylene meshes (3 × 3 cm) using an airbrush system. This yielded to homogenous and regular films that did not alter mesh shape or

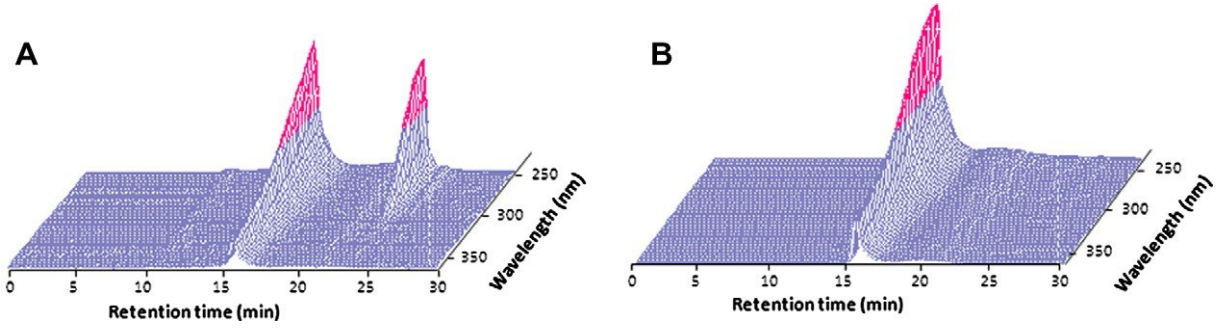

Fig. 1. 3-D SEC chromatograms of Bn_2-DTPA-PCL solutions in THF containing free Bn_2-DTPA (A) or Bn_2-DTPA-PCL (B).

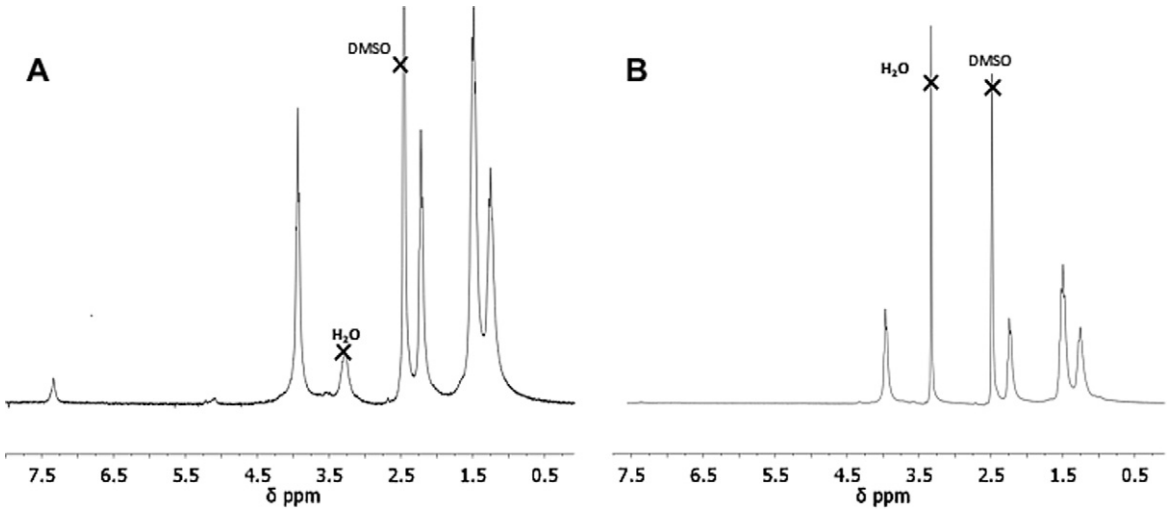

Fig. 2. ^{1}H NMR spectrum of Bn_2-DTPA-PCL (A) and DTPA-PCL (B) in d_6-DMSO.

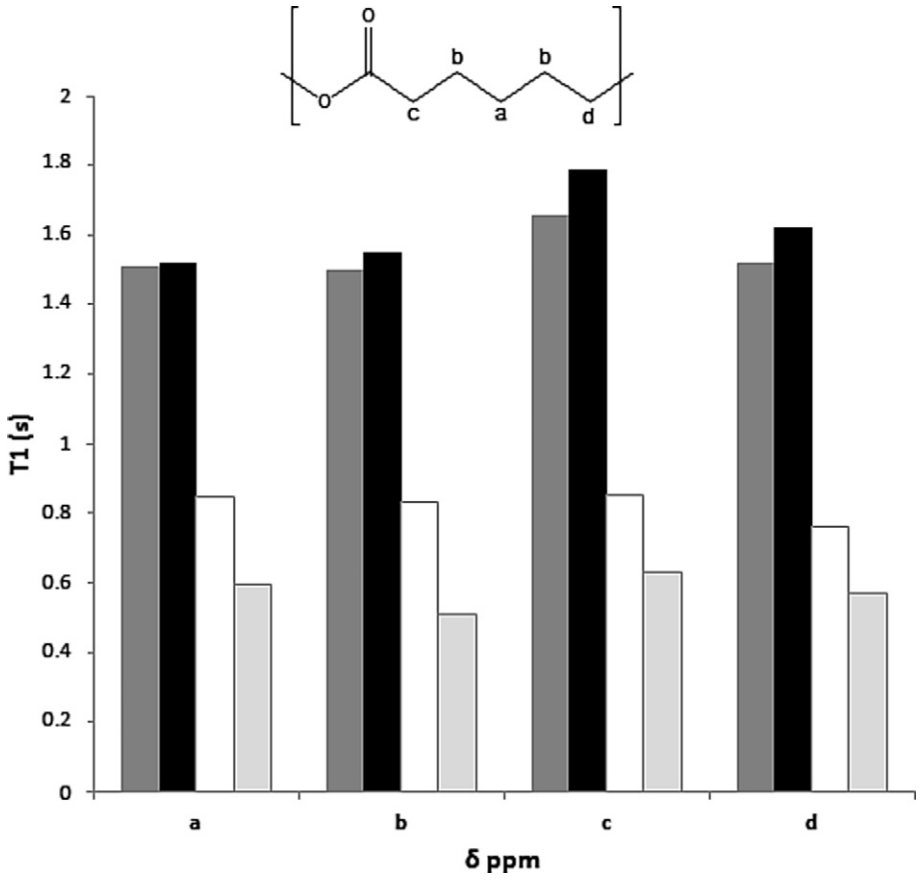

Fig. 3. Relaxation times (assigned by chemical shift) for protons in the polymer backbone of PCL (▨ and DTPA-PCL (■) (negative controls), compared with 0.3% (h) and 0.8% (▨ DTPA-Gd-PCL.

integrity (Supplementary data 3). DTPA-Gd-PCL was seen to possess appropriate filmogenic properties on polypropylene mesh without any breaking or peeling, and this was regardless of the amount of polymer sprayed on the meshes.

Fig. 4G shows that gadolinium-free coated mesh did not elicit any contrast enhancement. In comparison, the DTPA-Gd-PCL (Fig. 4H) coated mesh was clearly visible in the agarose gel. The mesh's ''whitening effect'' is due to positive T1 signal enhancement. No free gadolinium diffused into the medium, showing that it remained complexed to the polymer skeleton.

Similar studies on Magnevist®-coated meshes underlined the importance of the effective grafting of the contrast agent onto the polymer backbone. MR images of Magnevist® powder showed T1 signal enhancement in all the release media after a few minutes, resulting from the rapid diffusion of highly soluble free DTPA-Gd (data not shown).

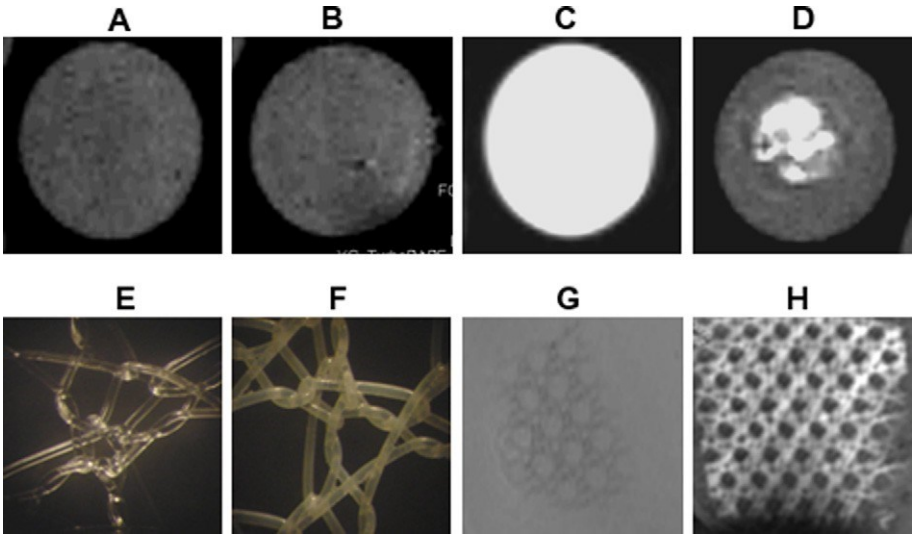

Fig. 4. MR images of polymers: PCL powder (A) and DTPA-PCL powder (B) as negative controls, a solution of Magnevist® as positive control (C) and DTPA-Gd-PCL powder (D). Optical microscope images of commercially available native mesh and DTPA-Gd-PCL-coated mesh (E and F) and their MR images (G and H).

3.2.3. In vitro stability of the DTPA-Gd-PCL chelate

In vitro stability studies were carried out in PBS to detect any release of free toxic gadolinium [35,36] and to evaluate long-term MR visualization (Fig. 5). To avoid adverse effects in the body, it was important to determine whether any gadolinium was released from the MRI-visible prosthesis. With regards to the removal of carboxylate group, one can postulate that the stability of the complex could be modified and, consequently, a stability study must be performed. Given that grafted polymers were not water-soluble and thermodynamic and kinetic constants are measured in aqueous solution, the stability of the complex was studied by titrating the gadolinium released in aqueous medium by ICP-MS (inductively coupled plasma-mass spectrometry).

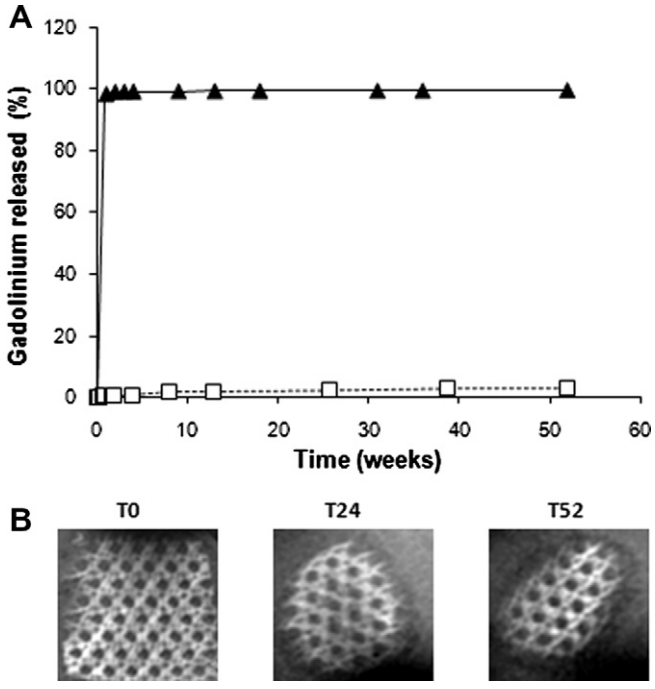

Fig. 5. (A) Release of gadolinium from a mesh coated with a mixture of Magnevist®/PCL (–N–) and from a mesh coated with DTPA-Gd-PCL (···□···). (B) MR images of DTPA-Gd-PCL-coated meshes at T0 and after 24 and 52 weeks of stability testing in PBS at 37 °C.

A control, based on a mixture of Magnevist® + PCL, was prepared containing non-grafted DTPA-Gd. This mixture was prepared to demonstrate that a simple dispersion of a contrast agent in a polymeric matrix cannot allow a long-term MRI visualization. Indeed, total release of the contrast agent was observed within a few days: 878 μg of the initial 885 μg of Gd were released in the first week. By contrast, grafting of the DTPA onto the polymer prevented the release of gadolinium. Indeed, only 7 μg of gadolinium were released in 12 months, which correspond to 3% of the initial amount of Gd on the coated mesh.

Moreover, this release is very insignificant compared to the suspected Gd^{3+} decomplexation after Gd-based contrast agent injections. In vitro studies performed in human serum suggested that up to 2% of Gd^{3+} were decomplexed from Magnevist® (corresponding to 3.1 mg $l^{-1}$of plasma) after only 15 days of incubation [37].

The persistence of T1 signal enhancement on DTPA-Gd-PCL coated meshes was also assessed. Fig. 5B shows that the MR signal was maintained for a period of at least 52 weeks. These results corroborate the gadolinium release data and suggest that an implantable medical device coated with DTPA-Gd-PCL could be visualized by MRI for at least 1 year.

It is important to specify that the MRI visualization of these meshes (3 × 3 cm) required the coating of 2 mg of polymer, thus corresponding to a maximum of 100 μg of gadolinium. This value is much lower than the required clinical amount of gadolinium injected in a patient before MRI scanning, which is ~1.5 g for Magnevist®.

3.3. In vitro cell cytocompatibility

Two studies were performed to assess the cytocompatibility of PCL-Gd-DTPA: an evaluation of human fibroblast adhesion and proliferation on polymer films to determine whether this polymer is suitable for cell culture, and an assessment of human fibroblast colonization on a coated mesh to mimic the wound healing process.

Fig. 6 shows the adhesion (15, 30 and 60 min.) and proliferation (1, 4 and 7 days) of human fibroblasts (HFBs) on DTPA-Gd-PCL compared to native PCL and TCPS. HFB adhesion and proliferation were quantified by MTT assay that reflects the number of living cells present on a surface at a given time. It may be concluded from Fig. 6A that the surface of the new MRI-visible polymer did not

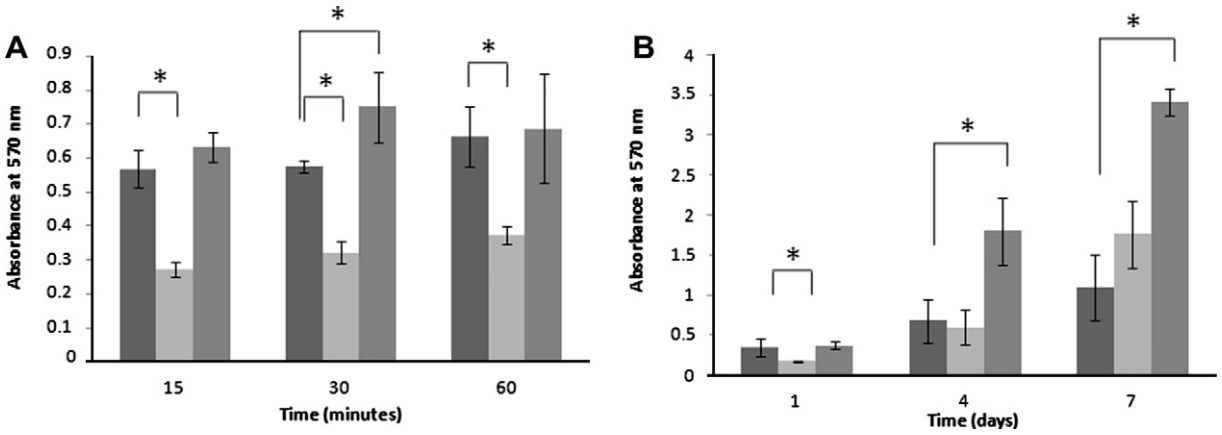

Fig. 6. MTT results illustrating cell viability on TCPS (positive control, ■) compared with PCL (■) and DTPA-Gd-PCL (■) films after adhesion (A) and proliferation (B) tests. The ω shows a statistical significant difference (ANOVA $p < 0.05$, Student–Newman–Keuls test).

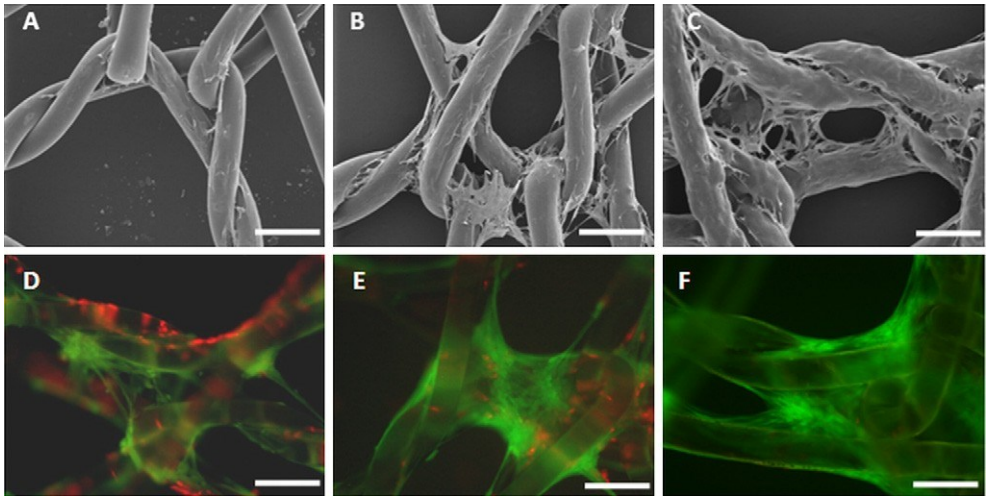

Fig. 7. SEM and fluorescent microscopy pictures of native PP meshes (A and D), PCL-coated meshes (B and E) and DTPA-Gd-PCL-coated meshes (C and F) after 5 days of proliferation. Live and dead staining (D, E and F) highlights viable cells (green) and dead cells (red) (scale bars represent 200 1m).

impede fibroblast adhesion. The fibroblasts rapidly adhered to TCPS and DPGA-Gd-PCL after only 15 min, and longer adherence times did not significantly increase the number of cells present on the surface. Cell adherence to native PCL was significantly lower, which may be due to PCL's marked hydrophobicity and the degree of crystallinity hampering the cell adherence process. Fig. 6B, illustrating HFB proliferation, shows better cell growth on DTPA-Gd-PCL than on TCPS and PCL. MTT results after 1, 4 and 7 days corresponded to 0.36, 0.68 and 1.1 for TCPS compared with 0.36, 1.8 and 3.4 for DTPA-Gd-PCL. DTPA-Gd-PCL would therefore appear to be suitable for the growth of human fibroblasts.

Fig. 7 shows SEM and fluorescent microscopy images of meshes after 5 days of HFB proliferation. As it can be seen in frame pictures A and D, taken after 5 days of incubation, native PP meshes were poorly covered by cells and most of the HFB present are red stained after live and dead staining, demonstrating a cytotoxic surface effect. No fibroblasts were attached to the surface of the mesh after 10 days (data not shown), indicating that native PP meshes are not prone to in vitro colonization. By contrast, after 5 days of HFB proliferation PCL- and DTPA-Gd-PCL-coated meshes were covered by extensively spread cytoplasm cells, a typical morphology of normal fibroblasts (Fig. 7B and C). After a 10-day incubation period, the coated meshes were almost entirely covered by cells (data not shown). These data were supported by vital cell staining after 5 and 10 days of incubation (after 5 days: Fig. 5D and F; after 10 days: data not shown). After 5 days, MRI-visible meshes were covered by HFB, as shown by an elongated green cytoplasm, without any signs of toxicity (no red staining). Cell morphology and viability were similar on PCL-coated mesh, though more red-stained HFB nuclei appeared to be present.

It may therefore be concluded, based on these in vitro cytocompatibility tests, that the surface of this new MRI-visible polymer did not reduce either the adherence or the proliferation of human fibroblasts, unlike TCPS or native PCL. Moreover, live and dead studies supported by SEM observations showed that viable and typically shaped fibroblast cells were colonizing the DTPA-Gd-PCL coated meshes.

4. Conclusion

We have described the synthesis of a new MRI-visible, PCL-based polymer for the visualization of implantable medical devices. This polymer was prepared by covalent grafting DTPA onto the PCL backbone, followed by the chelation of gadolinium onto the grafted DTPA. SEC, ^{1}H NMR and ICP-MS analyses confirmed that the DTPA-Gd complex was successfully attached to the PCL skeleton with a substitution degree of 0.5%. This MRI-visible polymer was then coated onto a commercially available polypropylene mesh. Sufficient gadolinium was grafted onto the polymer to induce a strong

and clear T1 contrast enhancement. A DTPA-Gd-PCL-coated polypropylene mesh was MRI-visible in vitro for at least 1 year and only a tiny proportion (<3%) of the chelated gadolinium grafted onto the polymeric backbone was released within this period. Moreover, in vitro cytocompatibility assessments demonstrated that this polymer may be used as a coating for implantable medical devices without any negative impact on cell proliferation. This study has demonstrated that a degradable MRI-visible polymer can be used to visualize medical devices in vitro by MRI. This progress could be a tool for surgeons to locate implantable medical devices by MRI. In order to confirm the great potential of this polymer in the long-term MRI visualization of medical devices, in vivo studies are under investigation to test the biocompatibility of this new polymer and to locate a DTPA-Gd-PCL-coated mesh after implantation in an animal.

Acknowledgements

The authors are grateful to Dr. Chantal Cazevieille (CRIC, University Montpellier I) for her technical assistance and interpretation of ultrastructural data, to Sylvie Hunger for ^{1}H NMR analyses and Dr. Olivier Bruguier (Geosciences, University Montpellier II) for his help in ICP-MS measurements. This work was partially supported by the ''Agence Nationale de la Recherche'' No. ANR-08-TECS-020-01.

Appendix A. Supplementary data

Supplementary data associated with this article can be found, in the online version

Appendix B. Figures with essential colour discrimination

Certain figures in this article, particularly Figs. 1, 4, and 7, are difficult to interpret in black and white. The full colour images can be found in the on-line version

References

[1] Langer R, Peppas NA. Advances in biomaterials, drug delivery, and bionanotechnology. AIChE J 2003;49:2990–3006.
[2] Langer R, Tirrell DA. Designing materials for biology and medicine. Nature 2004;428:487–92.
[3] Vert M. Polyvalent polymeric drug carriers. Crit Rev Ther Drug Carrier Syst 1986;2:291–327.
[4] Griffith LG. Polymeric biomaterials. Acta Mater 2000;48:263–77.
[5] Vert M. Bioresorbable polymers for temporary therapeutic applications. Angew Makromol Chem 1989;166:155–68.
[6] Vert M, Feijen J, Albertsson A, Scott G, Chiellieni E. Biodegradable polymers and plastics. R Soc Chem, Cambridge 1992;33:437–8.
[7] Fischer T, Ladurner R, Gangkofer A, Mussack T, Reiser M, Lienemann A. Functional cine MRI of the abdomen for the assessment of implanted synthetic mesh in patients after incisional hernia repair: initial results. Eur Radiol 2007;17:3123–9.
[8] Nottelet B, Coudane J, Vert M. Synthesis of an X-ray opaque biodegradable copolyester by chemical modification of poly (epsilon-caprolactone). Biomaterials 2006;27:4948–54.
[9] Boukerrou M, Mesdagh P, Yahi H, Crepin G, Robert Y, Cosson M. MRI evaluation of surgical pelvic floor repair. Gynecol Obstet Fertil 2006;34:1024–8.
[10] Lauterbu PC. Image formation by induced local interactions – examples employing nuclear magnetic-resonance. Nature 1973;242:190–1.
[11] van Geuns RJ, Wielopolski PA, de Bruin HG, Rensing BJ, van Ooijen PM, Hulshoff M, et al. Basic principles of magnetic resonance imaging. Prog Cardiovasc Dis 1999;42:149–56.
[12] Xu H, Othman SF, Magin RL. Monitoring tissue engineering using magnetic resonance imaging. J Biosci Bioeng 2008;106:515–27.
[13] Port M, Idee JM, Medina C, Robic C, Sabatou M, Corot C. Efficiency, thermodynamic and kinetic stability of marketed gadolinium chelates and their possible clinical consequences: a critical review. Biometals 2008;21:469–90.
[14] Bumb A, Brechbiel MW, Choyke P. Macromolecular and dendrimer-based magnetic resonance contrast agents. Acta Radiol 2010;51:751–67.
[15] Kramer NA, Donker HCW, Otto J, Hodenius M, Senegas J, Slabu I, et al. A concept for magnetic resonance visualization of surgical textile implants. Invest Radiol 2010;45:477–83.
[16] Stuber M, Gilson WD, Schar M, Kedziorek DA, Hofmann LV, Shah S, et al. Positive contrast visualization of iron oxide-labeled stem cells using inversion-recovery with ON-Resonant water suppression (IRON). Magn Reson Med 2007;58:1072–7.
[17] Chan KWY, Wong WT. Small molecular gadolinium(III) complexes as MRI contrast agents for diagnostic imaging. Coord Chem Rev 2007;251:2428–51.
[18] Aime S, Botta M, Fasano M, Terreno E. Lanthanide(III) chelates for NMR biomedical applications. Chem Soc Rev 1998;27:19–29.
[19] Weinmann HJ, Brasch RC, Press WR, Wesbey GE. Characteristics of gadolinium-DTPA complex: a potential NMR contrast agent. AJR Am J Roentgenol 1984;142:619–24.
[20] Kim JH, Park K, Nam HY, Lee S, Kim K, Kwon IC. Polymers for bioimaging. Prog Polym Sci 2007;32:1031–53.
[21] Bogdanov AA, Weissleder R, Frank HW, Bogdanova AV, Nossif N, Schaffer BK, et al. A new macromolecule as a contrast agent for Mr-Angiography – preparation, properties, and animal studies. Radiology 1993;187:701–6.
[22] Duarte MG, Gil MH, Peters JA, Colet JM, Elst LV, Muller RN, et al. Synthesis, characterization, and relaxivity of two linear Gd(DTPA)-polymer conjugates. Bioconjug Chem 2001;12:170–7.
[23] Kobayashi H, Kawamoto S, Jo SK, Bryant Jr HL, Brechbiel MW, Star RA. Macromolecular MRI contrast agents with small dendrimers: pharmacokinetic differences between sizes and cores. Bioconjug Chem 2003;14:388–94.
[24] Langereis S, de Lussanet QG, van Genderen MHP, Backes WH, Meijer EW. Multivalent contrast agents based on gadolinium-diethylenetriaminepentaacetic acid-terminated poly(propylene imine) dendrimers for magnetic resonance imaging. Macromolecules 2004;37:3084–91.
[25] Rebizak R, Schaefer M, Dellacherie E. Polymeric conjugates of Gd3+-diethylenetriaminepentaacetic acid and dextran. 1. Synthesis, characterization, and paramagnetic properties. Bioconjug Chem 1997;8:605–10.
[26] Tulu M, Geckeler KE. Synthesis and properties of hydrophilic polymers. Part 7. Preparation, characterization and metal complexation of carboxy-functional polyesters based on poly(ethylene glycol). Polym Int 1999;48:909–14.
[27] Mody VV, Nounou MI, Bikram M. Novel nanomedicine-based MRI contrast agents for gynecological malignancies. Adv Drug Deliv Rev 2009;61:795–807.
[28] Doiron AL, Chu K, Ali A, Brannon-Peppas L. Preparation and initial characterization of biodegradable particles containing gadolinium-DTPA contrast agent for enhanced MRI. Proc Natl Acad Sci U S A 2008;105:17232–7.
[29] Jiang XQ, Yu H, Frayne R, Unal O, Strother CM. Novel magnetic resonance signal enhancing coating material. Adv Mater 2001;13:490.
[30] Safinia L, Datan N, Hohse M, Mantalaris A, Bismarck A. Towards a methodology for the effective surface modification of porous polymer scaffolds. Biomaterials 2005;26:7537–47.
[31] Yang Y, Lee J, Cho M, Sheares VV. Synthesis of amine-functionalized diene-based polymers as novel gene delivery vectors. Macromolecules 2006;39:8625–31.
[32] Guo J, Jiang X, Hu Y, Yang C. Preparation of Gd3+-containing polymer complex as a novel magnetic resonance signal-enhancing coating material. J Mater Sci Mater Med 2003;14:283–6.
[33] Ponsart S, Coudane J, Vert M. A novel route to poly(epsilon-caprolactone)-based copolymers via anionic derivatization. Biomacromolecules 2000;1:275–81.
[34] Vonarbourg A, Sapin A, Lemaire L, Franconi F, Menei P, Jallet P, et al. Characterization and detection of experimental rat gliomas using magnetic resonance imaging. Magma 2004;17:133–9.
[35] Goulle JP, Saussereau E, Mahieu L, Bouige D, Groenwont S, Guerbet M, et al. Application of inductively coupled plasma mass spectrometry multielement analysis in fingernail and toenail as a biomarker of metal exposure. J Anal Toxicol 2009;33:92–8.
[36] Thakral C, Abraham JL. Nephrogenic systemic fibrosis: histology and gadolinium detection. Radiol Clin North Am 2009;47:841.
[37] Frenzel T, Lengsfeld P, Schirmer H, Hutter J, Weinmann HJ. Stability of gadolinium-based magnetic resonance imaging contrast agents in human serum at 37 degrees C. Invest Radiol 2008;43:817–28.